INL/CON-16-37835
PREPRINT

Three-Dimensional FIB/EBSD Characterization of Irradiated $HfAl_3$-Al Composite

Top Fuel 2016

Zilong Hua, Donna Post Guillen,
William Harris, Heng Ban

September 2016

The INL is a
U.S. Department of Energy
National Laboratory
operated by
Battelle Energy Alliance

Three-Dimensional FIB/EBSD Characterization of Irradiated $HfAl_3$-Al Composite

Zilong Hua[1], Donna Post Guillen[2], William Harris[2,3], and Heng Ban[1]

[1]*Utah State University, Logan, UT USA*
[2]*Idaho National Laboratory, Idaho Falls, ID USA*
[3]*North Carolina State University, Raleigh, NC USA*

Abstract. A thermal neutron-absorbing composite comprised of 28.4 vol% $HfAl_3$ intermetallic particles in an Al matrix, developed for use in a conductively cooled thermal neutron filter, will enable fast flux irradiation of materials and fuels in an existing pressurized water test reactor. In this paper, an EBSD-FIB characterization approach is used to observe the microstructural changes of the $HfAl_3$-Al composite in response to simulated long-term neutron irradiation. Using a focused ion beam (FIB), the sample was fabricated to 25µm × 25µm × 20 µm and mounted on a transmission electron microscopy (TEM) grid. A series of operations were carried out repeatedly on the sample's top surface to prepare it for scanning electron microscopy (SEM). First, a ~100-nm layer was removed by high voltage FIB milling. Then, several cleaning passes were performed on the newly exposed surface using low voltage FIB milling to improve the SEM image quality. The surface was then scanned by Electron Backscattering Diffraction (EBSD) to obtain a two-dimensional image. After 50 to 100 two-dimensional images were collected, the images were stacked to reconstruct a three-dimensional model using DREAM.3D software. Two such reconstructed three-dimensional models were obtained from samples of the original and post-irradiation $HfAl_3$-Al composite, from which the most significant microstructural change caused by neutron irradiation appears to be the size reduction of both $HfAl_3$ and Al grains. Possible causes include thermal expansion and related thermal strain from thermal neutron capture.

Keywords: neutron absorber, 3D microstructure, metal matrix composite

INTRODUCTION

Fast reactor technologies have drawn significant attention in recent decades because of the central role they are predicted to play in the attainment of a closed nuclear fuel cycle, in which spent fuels are recycled in order to harvest a larger fraction of their energy content; this not only minimizes nuclear waste but also provides a path for the disposal of nuclear weapon materials[1]. However, as a result of technical and political challenges and the widespread availability of uranium for conventional light water reactors, no fast reactors have been operational in the United States since 1994. Consequently, most fast flux irradiation testing for the development of Generation IV reactor fuels and materials has been conducted abroad.

The Idaho National Laboratory's Advanced Test Reactor (ATR) has been identified as a candidate site for the development of a fast flux irradiation testing facility within the United States[2]. This renewed interest in fast reactor technologies is in response to global pressures to minimize nuclear waste products while expanding overall nuclear energy production. The current design plan is called the Boosted Fast Flux Loop (BFFL), which simulates a fast flux environment within the light water reactor by surrounding experiment capsules with uranium silicide booster fuel and filtering thermal neutrons from reaching the test specimens[3]. This filtering is achieved using an $HfAl_3$-Al thermal neutron absorbing metal matrix composite material[4]. The $HfAl_3$ intermetallic particles have a large cross section for thermal neutron capture and experience significant heating during irradiation, while the Al matrix conducts this heat to nearby coolant channels. Moreover, both metals have good resistance to corrosion. Guillen et al. reported that a 28.4 vol% concentration of $HfAl_3$ is optimal to achieve a fast neutron flux of 10^{15} n/cm^2-s and a fast to thermal ratio of 40 within the test capsule[4].

Accurate thermal hydraulic modeling of the BFFL design scheme and reliable predictions of in-service lifetime require knowledge of the $HfAl_3$-Al composite's thermo-mechanical response to long-term

irradiation. Guillen et al. reported correlations for the temperature-dependent bulk thermal conductivity of the $HfAl_3$-Al material after irradiation in the ATR for 0, 1965.5, 3184.0, and 3984.6 megawatts days[5]. Finite element simulations performed on two-dimensional reconstructed cross sections of the material found that using asymptotic expansion homogenization (AEH) to calculate the bulk thermal conductivity yielded good experimental agreement at low temperatures, supporting the assumption that the material is homogeneous and isotropic on the micrometer scale[5]. However, limitations in current fabrication techniques will likely cause local inhomogeneities within the $HfAl_3$-Al composite that were not captured in these simulations. These defects could result in temperature fluctuations and possible thermal failures if the material exceeds the melting point of Al during operation. Thus, microstructure characterization of the composite material will be needed to inform future three-dimensional thermal analyses.

Three-dimensional electron backscatter diffraction (3D EBSD), which combines the precise sectioning attainable using focused ion beam (FIB) milling with the detailed crystallographic characterization provided by 2D EBSD, has become a cutting edge technique in microstructural studies. The 3D image is reconstructed from a series of 2D EBSD scans obtained at different depths within the sample using the DREAM.3D software package, which can be used for alignment of adjacent scans, cleanup of data with low confidence index values using the grain dilation method, and phase segmentation based on grain orientation mismatch[6,7]. In this manuscript, the procedure for applying the 3D EBSD technique to characterize the $HfAl_3$-Al composite is presented. Comparing the three-dimensional reconstructions of pre- and post-irradiation specimens will allow the irradiation-induced microstructural changes to be identified.

SAMPLE PREPARATION AND EXPERIMENTAL PROCEDURE

The $HfAl_3$ material was created using the centrifugal casting method; the details of fabrication and characterization can be found in previous publications[8-11]. With its phase examined and confirmed by X-ray diffraction (XRD), the $HfAl_3$ metal was ground into a powder and mixed with Al powder at 28.4 vol%, after which the $HfAl_3$-Al pucks were machined into millimeter-size disks through a hot press process. Observed by EBSD, most of the $HfAl_3$ and Al grains in the final sample had diameters less than 10 μm.

FIB milling using a FEI Quanta 3D FEG was used to fabricate several 25μm×25μm×35μm $HfAl_3$-Al samples. A 100 nm platinum layer was first coated to mark the target area. A high-voltage gallium beam was then used to melt and remove the surrounding materials and cut off the connection between the EBSD sample and the bulk, after adhering the sample to an Omni-probe using excessive platinum coating. Finally, the EBSD sample was mounted on a transmission electron microscopy (TEM) grid, as in Figure. 1 below. SEM/EBSD was used to remove layers of material and obtain grain information. Since EBSD cannot differentiate between the $HfAl_3$ and the aluminum, it is necessary to use Energy Dispersive Spectrometry (EDS). Data from a few slices is reconstructed to ensure that the data quality is acceptable before obtaining additional slices. Typically, it is desired to obtain ten scans (or slices) through a grain. It is estimated that four scans per grain is the minimum number that would produce sufficient data for an acceptable 3D reconstruction of this two-phase material.

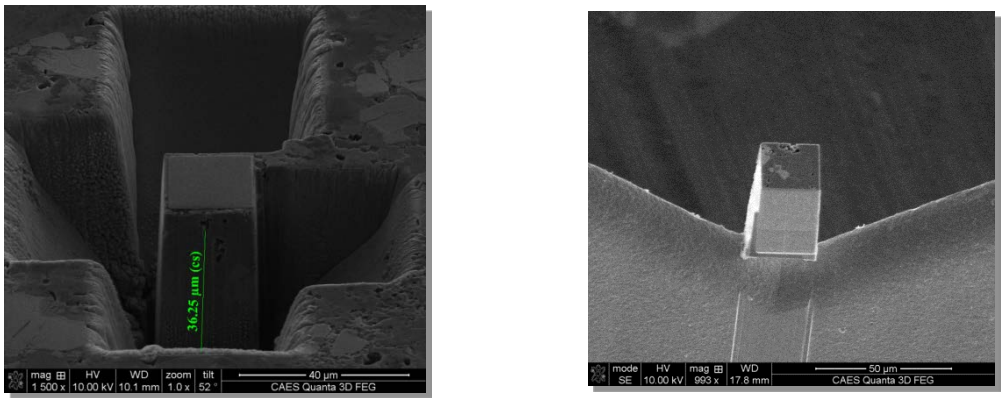

FIGURE 1**.** SEM images of the micrometer-scale sample (a) before the sample was separated from the bulk material and (b) after mounting on the grid.

A series of 2D EBSD scans is necessary for the 3D reconstruction. Approximately 100 nm of material was removed during each serial section. After each FIB milling step, a 2D EBSD scan is obtained on the newly exposed surface. Because the DREAM.3D software tool requires equal resolution in all dimensions, the thickness of the layer removed by FIB milling (the z-resolution) was set to the 2D EBSD scan step size (the x- and y-resolutions); this was set to 100 nm based on the smaller grain size in the sample.

The quality of the 3D reconstruction depends greatly on the quality of the 2D scans. High-voltage FIB milling removes the target layer effectively but usually leaves a rough surface that significantly reduces EBSD scan quality. The FIB employs a gallium source, which (at higher power levels) damages the material and hinders the collection of a diffraction pattern on the $HfAl_3$ intermetallic particles. A series of passes at lower power levels was performed after high power milling to minimize material damage from the gallium ions. While low-voltage fine FIB milling greatly improves the surface quality, the procedure can takes several days to accomplish. After numerous tests, a combined series of high/low-voltage FIB milling operations was found to balance these requirements. The details, which consist of an initial high voltage milling step followed by five low voltage cleaning passes, are outlined in Table 1. The sample must be tilted during low-voltage FIB millings according to the voltage/current settings. The EBSD images before and after low-voltage milling are given in Figure. 2 to illustrate the improvement in image quality, particularly with respect to the $HfAl_3$ grains.

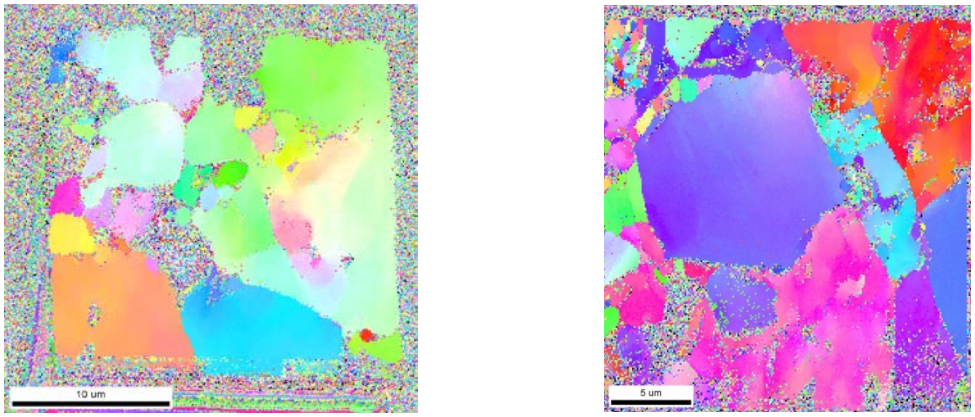

FIGURE 2**.** Examples of 2D EBSD scans with poor (left) and improved (right) image quality.

TABLE 1. FIB operating parameters.

	Voltage (kV)	Current (pA)	Sample tilt angle
0 (high-vol milling)	30	500	0

1	5	77	3
2	5	48	6
3	2	27	10
4	2	16	10
5	2	8.9	10

The open source software package DREAM.3D was used to stack the 2D EBSD scans and generate a three-dimensional reconstruction. In addition to aligning the scans, DREAM.3D can modify the position and phase/orientation information of grains by making comparisons between neighboring grains. The level of modification can be adjusted in the corresponding DREAM.3D filters to further improve the quality of the reconstruction. In particular, the confidence indices generated during the EBSD data collection can be used to remove data that is of poor quality, usually by enforcing a lower confidence threshold. Subsequently, those data points are replaced by assigning the missing crystal orientation values (Euler angles) with the surrounding values using the dilation method. Visualization was performed using the ParaView application which allows visualization of arbitrary slices through the reconstructed volume.

RESULTS AND DISCUSSION

EBSD-generated 3D models of the $HfAl_3$-Al composite material before and after neutron irradiation are presented in Figure. 3. In both models, the Al grains have better image quality than the $HfAl_3$ grains, likely because the $HfAl_3$ grains are more difficult to remove and therefore leave a rougher surface after FIB milling. It was observed that the EBSD collection software usually gives high confidence indices and fit values for Al grains but low values for $HfAl_3$ grains. Although low-voltage FIB milling improved $HfAl_3$ grain confidence indices, this did not prove sufficient to provide a high quality image.

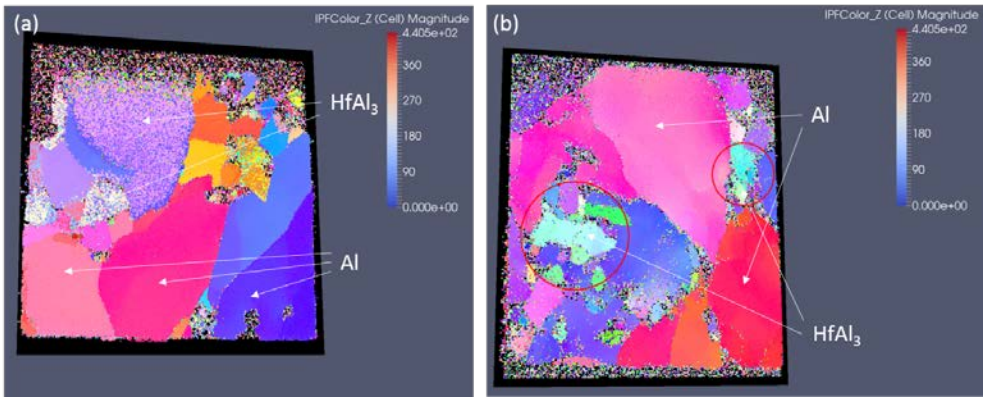

FIGURE 3. Sections of 3D reconstruction models: (a) unirradiated, and (b) irradiated

The number and average diameter of Al grains is found to be larger, in both 3D models, than those of the intermetallic grains. In this context, the diameter is taken to be the diameter of a sphere of equivalent volume as the feature. Particularly, in the sample before irradiation, only 1 $HfAl_3$ grain with diameter greater than 5 µm and 2 to 3 $HfAl_3$ grains with diameters of 2 µm are found (Figure. 4); as a comparison, at least 4 large Al grains with diameters of 5 to 10 µm and another 5 to 10 smaller Al grains with diameters of 2 to 5 µm can be seen.

When interpreting this data, it must be noted that the grain diameters obtained from the reconstruction are generally skewed toward lower values. This is because grains that intersect the sample boundary do not have their full volumes recorded. Moreover, larger grains are more likely to intersect the boundary and have their volumes underestimated. Due to the small region that was studied, exclusion of such features would have significantly reduced the amount of data available for this analysis. Therefore, those features were retained; because the same limitation is present for both the unirradiated and irradiated microstructures,

comparisons between the two should remain representative of data available from a larger sample. However, for either data set, the statistical distribution of the phases should not be taken as representative of the bulk.

Figures. 4 to 6 contain SEM images for the unirradiated 28.4 vol% material. Figure. 4 shows a SEM image that contrasts the $HfAl_3$ particles (colored in red) with the aluminum matrix (colored in gray). Figure. 5 shows a grain size histogram for the aluminum matrix. Figure. 6 shows an inverse pole figure (IPF) of the aluminum microstructure. In this image, the $HfAl_3$ is not indexed (shown in black).

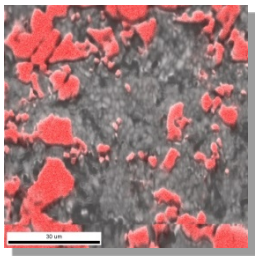

FIGURE 4. SEM image showing the $HfAl_3$ particles in red.

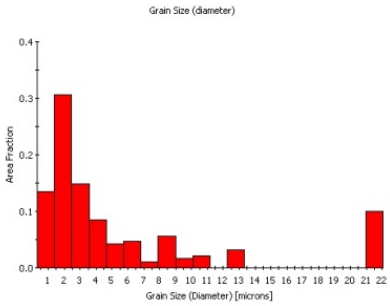

FIGURE 5. Grain size distribution of aluminum matrix in 28.4 vol% unirradiated composite.

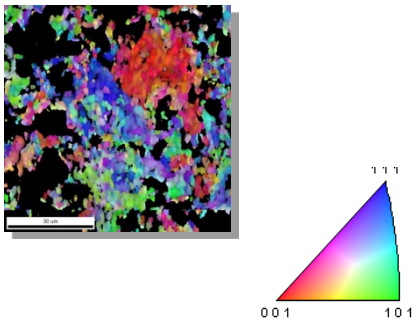

FIGURE 6. IPF of aluminum microstructure.

During post-irradiation examination, similar difficulties were encountered when performing SEM with electron backscatter diffraction (EBSD) and electron dispersive spectroscopy (EDS). While the aluminum indexes nicely, the $HfAl_3$ does not. Considerable resources have been spent on SEM/EDS analysis without much success. The instrument vendor was consulted and even provided several new libraries, but the Kikuchi patterns obtained do not match any of those in the libraries. The images in Figure. 7a and 7b compare an inverse pole figure (IPF) with a greyscale image. Figure. 7a shows the noise in the intermetallic regions due to the low confidence index at those points. Figure. 7b shows the overall grain structure, in which grains composed of the matrix material and intermetallic appear as a lighter or darker shade of gray, respectively. It is impossible from these images to ascertain the local orientation texture of the intermetallic. Figure. 8 shows a 3D microstructural reconstruction of the poorly indexed grains.

According to the literature, the intermetallic particles should index as tetragonal[8], but the Kikuchi patterns suggest a cubic structure. If the intermetallic indeed has a cubic structure, then there is likely some type of metastable phase that forms in the material. The material was carefully fabricated to crystallize in the low-temperature $D0_{23}$, rather than high-temperature $D0_{22}$, phase. The tetragonal unit cell of type $D0_{23}$ contains four $HfAl_3$ molecules with a value of ~ 4 for the axis ratio (c/a)[9]. It is well known that the EBSD patterns between the FCC (Fm3m, Al) and tetragonal (I4/mmm, Hf-Al) crystal systems do not differ greatly, such as those differences normally seen between a cubic and hexagonal system.

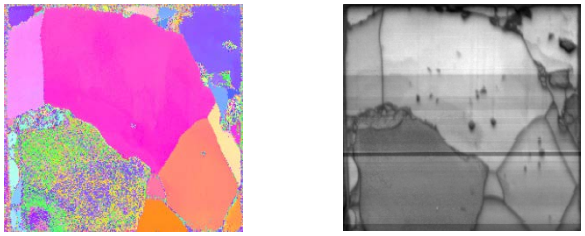

(a) (b)

FIGURE 7. (a) IPF showing inability to assess local orientation texture for $HfAl_3$ grains, (b) greyscale image showing overall grain structure.

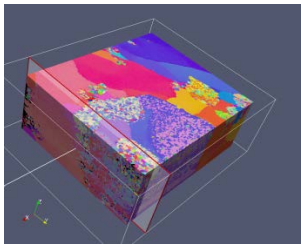

FIGURE 8. 3D microstructural reconstruction of noisy images.

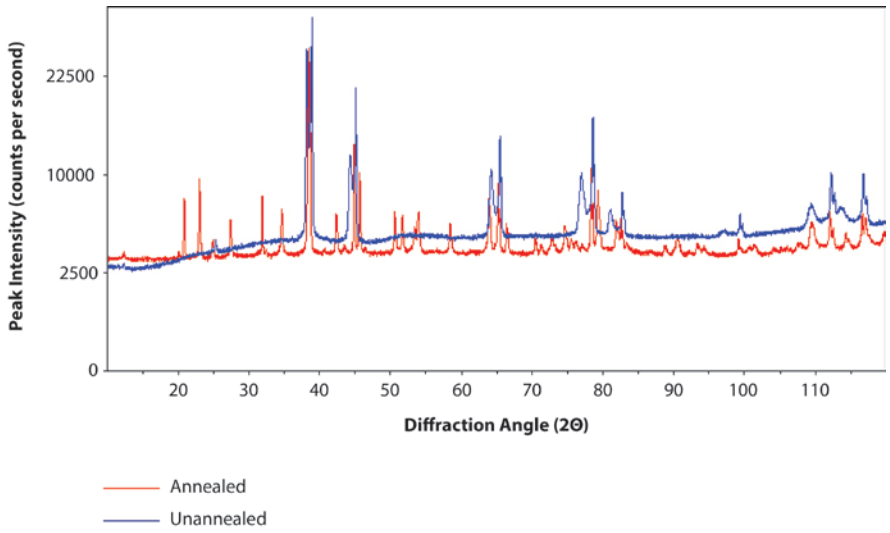

FIGURE 9. XRD of unannealed versus annealed irradiated specimen.

Figure. 9 shows the results of XRD on the irradiated material before and after annealing. The flatter profile of the unannealed sample is indicative of radiation-induced changes occurring in the material; this phenomenon is reported in greater detail by Guillen et al[5].

Future work includes beamline studies to obtain information on lattice parameters, coordination chemistry, distances, coordination number, species of the neighbors of the absorbing atom (i.e., Hf), etc. The high intensity and tunability of synchrotron x-rays make possible many powder diffraction experiments that are not practical or possible with a laboratory source. The low divergence of the synchrotron beam with a highly monochromatic beam allows extremely high resolution, whereas the high intensity provides much greater sensitivity to weak peaks or minor phases. Thus, it is possible to utilize synchrotron-derived data for much more accurate phase determination studies and for the solution and refinement of structures.

Comparing the sample reconstructions before and after irradiation, the grain size of $HfAl_3$ seems to be reduced significantly. All $HfAl_3$ grains in the post-irradiation model have diameters less than or comparable to ~1 µm. We have presented supporting, though not conclusive, evidence that average $HfAl_3$ grain size is reduced following simulated long-term irradiation. First, the $HfAl_3$ intermetallic phase in the post-irradiation 3D model appears in the form of small-grain clusters. This is in contrast to the unirradiated 3D model, where such clustering is not observed; rather, several large $HfAl_3$ grains are found to contain most of the $HfAl_3$ phase. As they are fabricated from the same bulk material, the form and structure of the $HfAl_3$ grains in the two models should be similar. A possible explanation for this phenomenon is recrystallization of the intermetallic phase in response to thermal expansion and related strain during neutron capture-induced internal heating. Additionally, the orientation of some Al grains in the post-irradiation 3D model appears to change slightly near a boundary with a neighboring $HfAl_3$ grain, which may indicate deformation of the Al lattice in response to thermal strain. Lastly, the grain size of the post-irradiation sample would be expected to increase due to the recovery process activated by heating from neutron capture. The as-run thermal analysis indicates that this specimen had an average temperature of 398K during irradiation with 402K as the bounding temperature. If the grain sizes of different samples are similar, a reasonable explanation of the seemingly reduced grain size of $HfAl_3$ is grain subdivision activated by the irradiation.

A larger scale 3D model is needed to support these claims. Unfortunately, due to the time-consuming nature of low-voltage FIB milling, it is impractical to perform similar 3D reconstructions on a sample significantly larger than those used in this study. Moreover, the size limitation of the reconstructed models also weakens the representation of the 3D EBSD samples to the entire composite material. As in the further

FEA thermal analysis, both the original and post-irradiation 3D models will be loaded into the FE analysis software MOOSE[12] as basic elements for the macroscale fast neutron absorber model assembling, from which the thermal performance of the absorber will be analyzed and predicted, this limitation needs to be carefully treated and relative optimization are necessary before the FEA analysis.

An alternative approach is to perform 2D EBSD at larger scale to examine the general 2D distribution of the $HfAl_3$. By comparing the volume % of current 3D EBSD models to the one of the entire composite material, a recipe to mix the 3D EBSD samples and pure Al/$HfAl_3$ elements as "fillers" in the FEA software can be proposed. Furthermore, different repeat patterns of 3D EBSD samples and fillers can be tested, with different $HfAl_3$ grain/Al grain/defects density, and corresponding performance variation can be studied.

Several 100μm × 100μm 2D EBSD images were obtained on both irradiated and unirradiated samples. Unfortunately, Al grains of the unirradiated sample cannot be correctly indexed by the software, which appears as noise areas in the images, and thus these images (at least for the unirradiated sample) cannot be used to decide the structures as described above, yet. The possible reason of the failure of indexing Al grains is that Silica solution used with vibratory polisher embeds into the porous oxidation layer of Al grains and causes a rough surface. Polished in the air environment, Al grains of the unirradiated sample are found containing Si and O on the surface by EDS. As a comparison, no extra element is found on Al grains of the irradiated sample, which was polished in the Ar environment. Observed by SEM, the irradiated sample surface is also apparently smoother than the one of the unirradiated sample. However, the grain diameter change of $HfAl_3$ were still noticed from images of two samples. Briefly, the number of grains with diameter larger than 10 μm is reduced by more than 50% after irradiation (averaged in each image), and more clusters of small $HfAl_3$ grains are found in the irradiated sample. It repeats part of our previous findings of the grain subdivision phenomena from the comparison of 3D reconstructed models of two samples, and will be more persuasive if Al grains can be indexed.

One special case of the relative position of $HfAl_3$/Al grains is shown in Figure. 10, where an Al grain is surrounded by multiple $HfAl_3$ grains. The probability of such a situation is hard to predict, but if Al grains are trapped in $HfAl_3$ grains, the generated thermal flux from $HfAl_3$ will not be conducted effectively and a local maximum temperature may be reached. In initial design with assuming $HfAl_3$ averagely distributed in the matrix, using an overall thermal conductivity of the $HfAl_3$ (40~50 W/m/K, measured by laser flash technique)[5], the simulation shows that the maximum temperature inside the absorber material is ~224 deg C, well below the melting point of Al (660 deg C). But with this sandwich structure, the local temperature may be far beyond the predicted temperature. If it surpasses the melting point of Al, the situation will become more complicated.

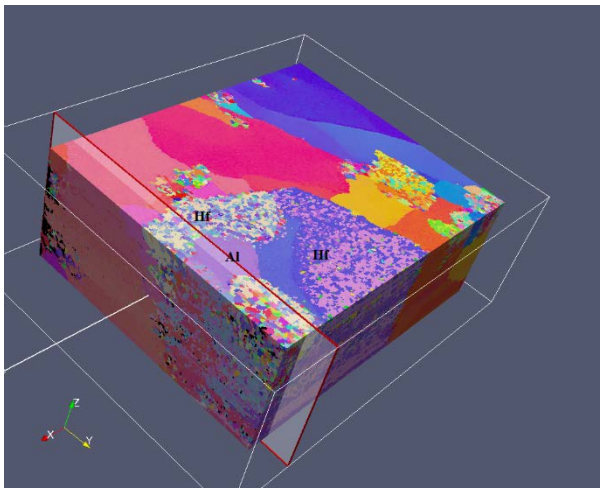

FIGURE 10. The 3D recontruction model to show the Al grain surrounded by $HfAl_3$ grains.

CONCLUSION

In order to simulate the fast reactor environment in an existing LWR, a new thermal neutron absorbing material, comprised of $HfAl_3$ particles and Al matrix has been developed. The microstructure of the material before and after neutron irradiation has been characterized using a 3D EBSD technique. Low-voltage FIB milling was found to improve the image quality of the EBSD scans. The neutron irradiation seems to cause the large $HfAl_3$ grains to break into small ones due to thermal neutron absorption and related thermal strain. In the next stage of this study, the reconstructed 3D model will be loaded into FEA software to assemble the macroscale thermal neutron absorber model and perform thermal analysis. The limitation due to the 3D EBSD sample size in the FEA and corresponding solutions are discussed.

ACKNOWLEDGMENTS

This work was supported under the auspices of the Nuclear Science User Facility by the DOE Office of Nuclear Energy, under DOE Idaho Operations Office Contract DE-AC07-05ID14517 and performed at the Center for Advanced Energy (CAES) Studies Microscopy and Characterization Suite. The researchers gratefully acknowledge Jatuporn Burns, who provided oversight and training on the instruments and Bradley Fromm for his assistance with the reconstruction procedure development.

REFERENCES

1. A.E. Walter, D.R. Todd, and P.V. Tsvetkov: *Fast Spectrum Reactors*, Springer, New York, 2012, pp. 3-8.

2. W.F. Skerjanc and G.R. Longhurst: Report No. INL/EXT-05-00263, Idaho National Laboratory, Idaho Falls, ID, July 2005.

3. G.R. Longhurst, D.P. Guillen, J.R. Parry, D.L. Porter, and B.W. Wallace: Report No. INL/EXT-07-12994, Idaho National Laboratory, Idaho Falls, ID, 2007.

4. D.P. Guillen and J.E. Fisher: Report No. INL/EXT-05-00446, Idaho National Laboratory, Idaho Falls, ID, November 2005.

5. D.P. Guillen and W.H. Harris. Measurement and Simulation of Thermal Conductivity of Hafnium Aluminum Thermal Neutron Absorber Material. 2016. Metallurgical and Materials Transactions E. DOI: 10.1007/s40553-016-0076-y.

6. M. Groeber, S. Gosh, M. D. Uchic, and D. M. Dimiduk. A framework for automated analysis and simulation of 3D polycrystalline microstructures. Part 1: Statistical characterization. 2008. Acta Materiala. 56, 1257-1273.

7. M. Groeber, S. Gosh, M. D. Uchic, and D. M. Dimiduk. A framework for automated analysis and simulation of 3D polycrystalline microstructures. Part 2: Synthetic structure generation. 2008. Acta Materiala. 56, 1274-1287.

8. S.K. Das, Chapter 8, Al-Rich Intermetallics in Aluminum Alloys, in *Structural Application of Intermetallic Compounds*, Edited by J.H. Westbrook and R.L. Fleischer, 1995, John Wiley & Sons, Ltd.

9. P. Wodniecki, et al., The Hafnium Aluminides $HfAl_3$ and Hf_2Al_3 Studied by Perturbed Angular Correlations with ^{181}Ta and ^{111} Cd Probes, *J. Alloys Compd.* 312 (2000) 17-24.

10. G. Balducci, et al., Thermodynamic study of intermetallic phases in the Hf-Al system, in *Journal of Allows and Compounds*, 220 (1995) 117-121

11. O. Levy, et al., Hafnium binary allows from experiments and first principles, in *Acta Materiala*, 58 (2010) 2887-2897.

12. D. Gaston, C. Newman, G. Hansen, and D. Lebrun-Grandie: Nucl. Eng. Des., 2009, vol. 10, pp. 1768-1778.